Title
Longitudinal Metabolic Changes in Premature Newborns

Author
Phillips, Elizabeth Dorothy

Publication Date
2015

Peer reviewed|Thesis/dissertation

Longitudinal Metabolic Changes in Premature Newborns

by

Elizabeth Phillips

THESIS

Submitted in partial satisfaction of the requirements for the degree of

MASTER OF SCIENCE

in

Biochemistry and Molecular Biology

in the

GRADUATE DIVISION

of the

UNIVERSITY OF CALIFORNIA, SAN FRANCISCO

Dedication

First, I would like to thank my parents for their unfailing love and support, and for the emphasis on education that they have maintained throughout my life. I literally would not be here without you.

I am deeply grateful for the myriad opportunities that have been made available to me here at UCSF. I would first like to thank my advisor, Dr. Duan Xu, for all his help and support over the last year. His levity and good humor (and lab meeting cookies!) have made it a pleasure to work on this project, and he has taught me more than I could ever have expected about magnetic resonance, pediatric neurology, and research in general.

I would also like to thank Dr. Yan Li for her endless patience and the many long hours she spent teaching me the ways of spectroscopy processing. I would have had a much harder time making sense of the data I acquired after processing without the gracious assistance and infinte wisdom of Dr. Hosung Kim, who helped me throughout the analysis portion of this project. For her valuable instruction in image processing, and for her help and support throughout this project, I would like to thank Dr. Sarah Nelson.

Thank you to Andrew Leynes, honorary Emperor of China Basin, for always patiently answering my coding questions and for helping me troubleshoot on numerous occasions. Thank you also to Adam Elkhaled for sharing his extensive knowledge of brain spectroscopy.

Dr. Jim Barkovich and Dr. Dan Vigneron have been generous with their time, supporting and advising me as members of my Thesis Committee. Thank you to Dr. Olga Tymofiyeva for her support and encouragement, and her unfailing positive attitude.

I would also like to thank Dr. David Saloner, Dr. Alastair Martin, Melinda Parangan-Chu, Robert Smith, and all my wonderful classmates for making my experience in the MSBI program an exceptional one.

This paper was typeset with LaTeX on www.overleaf.com

Longitudinal Metabolic Changes in Premature Newborns

Elizabeth Phillips

Abstract

Purpose: This study aims to investigate metabolic patterns in the brain during early neurodevelopment.

Methods: Spectroscopic data from 35 high-quality single-voxel spectroscopy scans performed on a total of 27 participants was processed and analyzed. These scans were performed as part of a study to investigate effects of preterm birth on neurodevelopment at UCSF.

Results: An increase in the N-Acetyl Aspartate/Creatine ratio and a decrease in both Choline/Creatine and *myo*-Inositol/Creatine with increasing age were found to be statistically significant.

Conclusions: The decrease in *myo*-Inositol was consistent with previous findings of a decrease in *myo*-Inositol concentration from birth to 5 years of age. This decrease may be due to myelin maturation and a reduction in cell turnover, but further investigation is needed to evaluate this hypothesis.

Contents

List of Figures

1 Background

The human brain undergoes rapid growth and development beginning in the third trimester of pregnancy and throughout childhood[1]. During this period, the brain is especially vulnerable to injury. Preterm birth is the most common cause of infant death and is the leading cause of long-term disability related to the nervous system in children. In 2012, preterm birth affected more than 1 of every 9 infants born in the United States[2]. Globally, an estimated 15 million babies are born prematurely every year, of whom almost 1 million will die due to complications[3]. Extreme prematurity of 22 to 25 weeks post-menstrual age (PMA) is associated with an overall mortality rate of $\geq$50%. High rates (17-59%) of severe neurodevelopmental disabilities occur among survivors[4].

1.1 Thalamus

The thalamus is a deep gray matter structure that consists of axonal fibers projecting to the entire cerebral cortex. [5] Signals relayed through the thalamus are transmitted throughout the brain and to the brainstem and spinal cord[6]. One of the major subcortical structures, the thalamus provides anatomical support for sensorimotor and higher-level cognitive functions[5]. Critical to integration of neural connections, the thalamus is thought to undergo metabolic maturation and dendritic arborization earlier than cerebral cortical regions[7][8].

In previous studies, it has been demonstrated that injury to the basal ganglia/thalamus regions was associated with the most impaired motor and cognitive outcome at 30 months when compared to a watershed pattern of injury involving mostly white matter[9].

1.2 Spectroscopic Imaging

^{1}H MR spectroscopy can provide valuable insight into the normal development of the perineonatal brain[10][11]. Quantitative information about the concentrations of brain metabolites can inform clinical assessment of prognosis by providing specific information about

type(s) and location(s) of tissue damage. In cases of preterm birth, detailed information about the metabolic concentrations and changes that occur over the course of development may provide greater insight into the physiological causes of disability associated with preterm birth, and may allow for more accurate prognosis of survival and risk of developmental disability.

1.3 Metabolites

1.3.1 *myo*-Inositol

The spectroscopic signal at 3.62 ppm is specific for cis-1,2,3,5-trans-4,6-cyclohexanehexol, also known as *myo*-Inositol (mI), without inclusion of other inositol stereoisomers or derivatives[12]. The most prominent stereoisomer of inositol, mI is one of the most abundant metabolites in the human brain. Found primarily in astrocytes, mI is considered a marker of immature myelination and glial cell proliferation[8][6]. mI is involved in hormone response pathways and protein-kinase C activation, it is a key precursor of the membrane phospholipid phosphatidyl inositol [13][14], and it is involved in the formation of myelin sheet structures[15]. mI can also function as an osmolyte; during periods of osmotic stress, osmotic balance is preserved via mI transport across the plasma membrane[16][14]. The concentration of mI, like choline (Cho), is expected to change in response to altered membrane metabolism or damage to cell membranes[13].

mI levels in the brain are elevated during the neonatal period, and have also been shown to be elevated in a variety of brain disorders (e.g. autism spectrum disorder, attention deficit hyperactivity disorder, [5] and hypoxia [15]). Conversely, a significant correlation between low language scores on 2-year-old BSID-III and decreased levels of mI on 1-year-old brain spectroscopy has previously been demonstrated[17].

1.3.2 N-Acetyl-L-Aspartate

The most prominent peak of the ^{1}H spectrum in the brain is the signal from the three equivalent protons on the acetyl group of N-Acetyl-L-Aspartate (NAA), which resonate at 2.0 ppm[13]. Because NAA is synthesized in neurons and diffuses along axons, it is interpreted as a marker of density of mature neurons and axons in the developing brain[13][8]. In neurons, NAA is synthesized within mitochondria[18], then combined with L-glutamate to form N-acetylaspartylglutamate (NAAG), which is then hydrolyzed back to NAA and L-glutamate by astrocytes. NAA is further hydrolyzed in oligodendrocytes to L-aspartate and acetate. This metabolic compartmentalization, wherein anabolic products of neurons are specifically targeted to oligodendrocytes and astrocytes, suggests that these substances may play an important role in cell-specific glial signaling [19].

1.3.3 Choline

The next prominent peak of the ^{1}H spectrum in the brain is the complex Choline (Cho) peak at 3.2 ppm, which consists of signal from several choline-containing compounds, most notably phosphocholine (PC) and glycerophosphocholine (GPC)[18][13]. Choline is present in phosphatidylcholine and sphingomylein, phospholipids that are abundant in cell membranes, including myelin. Therefore, the Cho peak is considered a marker of cell proliferation and signaling of cell membranes, including myelin sheaths[13].

1.3.4 Creatine

Next to the Cho peak, at 3.0 ppm, is the third prominent peak found in the ^{1}H spectrum in the brain: Creatine (Cre). This peak includes signal from phosphocreatine (PCr) and free creatine (fCr) in approximately equal contributions. PCr and fCr participate in rapid chemical exchange, replenishing ATP stores if needed, and therefore Cre concentration is representative of metabolic activity in the brain[13].

2 Hypothesis

mI levels have been shown to be elevated in the neonatal brain compared with adult levels, and a decrease in mI concentration over the course of early infancy has been demonstrated [8][13][18]. It is important to establish a normal pattern of changes in mI concentration across preterm brain development. The aim of this study is to assess changes in *myo*-Inositol concentration in the thalamus in relation to neonatal maturation in preterm newborns.

3 Methods

3.1 Patient Selection

Patients were enrolled through the Prematurely born neonate MRI (PreMRI) study, which has been ongoing at UCSF since 1998 [20]. Short-TE Single Voxel Spectroscopy (SVS) from 71 scans from a total of 48 patients was available starting in July 2012. Data from 35 scans performed on 27 patients were used in analysis; most of the excluded spectra were of insufficient quality due to either poor shimming or reduced quality as a result of patient motion. Coil sensitivity maps and spectral data were analyzed using LC Model[21], which performs automatic quantification, and peak width (full-width at half maximum) and signal-to-noise ratio (SNR) were recorded.

3.2 Image Acquisition

This study was approved by the Institutional Review Board, and informed parental consents were obtained for all infants enrolled.

The first MRI scans were performed as soon as the newborns were clinically stable for safe transport to the MRI scanner. In 19 of these patients, a second MRI scan was performed just before discharge or transfer from the hospital. All studies were performed on a 3-Tesla

General Electric Discovery MR750 system (GE Medical Systems, Waukesha, WI, USA) using an 8-channel head coil (GE 8HRBrain) at UCSF Mission Bay Medical Center. A neonatologist in the MR suite monitored the newborns during the scans.

The MR sequence performed for single-voxel spectroscopy (Point REsolved SpectroScopy, or PRESS) used echo times (TE) of 30 and 35 ms and repetition time (TR) of 1500 ms. The spectral width was 5000 kHz centered on water. A standard PRESS pulse sequence timing diagram is shown in Figure 1.

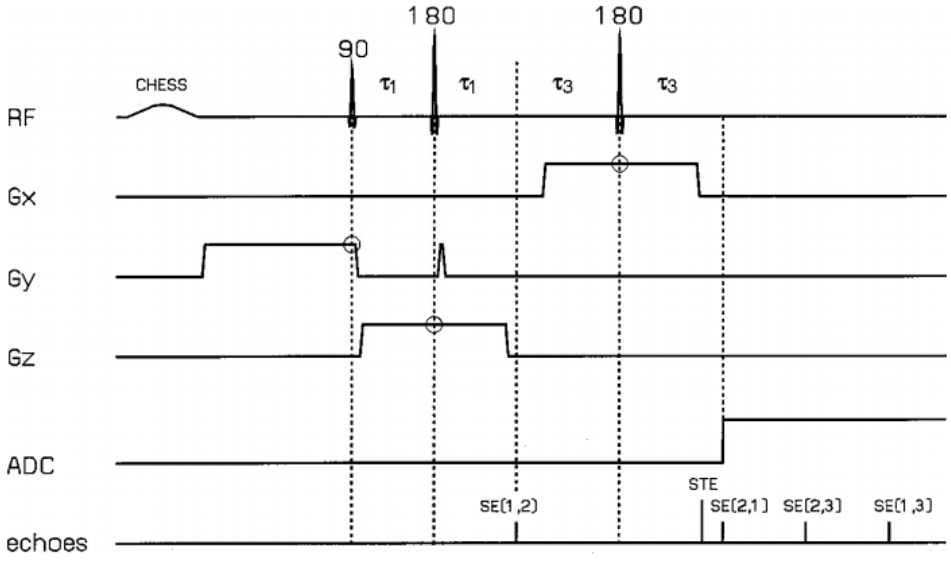

Figure 1: PRESS Timing Diagram

Short echo times were used in order to obtain greater signal from mI, which is not distinguishable at longer echo times due to inadequate SNR, as demonstrated in Figure 2, which was created with the SIVIC Software framework[22]. Use of a shorter echo time reduces T_2 signal loss due to spin dephasing. Certain metabolites like mI and glutamine+glutamate (Glx) have short T2 relaxation times (mI T_2 = 196ms)[23] due to strong J-coupling, which effectively decreases signal over the time evolution of the spin system. Echo times of 30-35 ms have been chosen to give both a coherent phase and high SNR.

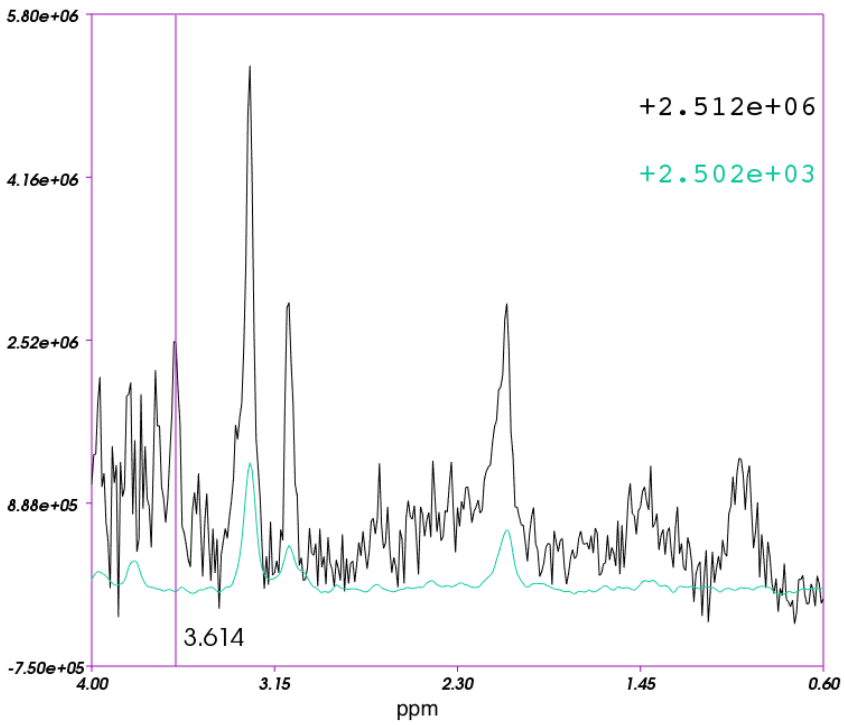

Figure 2: Comparison of Raw Spectra at TE = 35ms (black) and TE = 288 (green)

The voxel for the SVS acquisition was placed according to protocol, in a position intended to include as much of the thalamus, and as little extra-thalamic tissue, as possible. Typical voxel placement is demonstrated in Figure 3, in the a. axial, b. coronal, and c. sagittal planes.

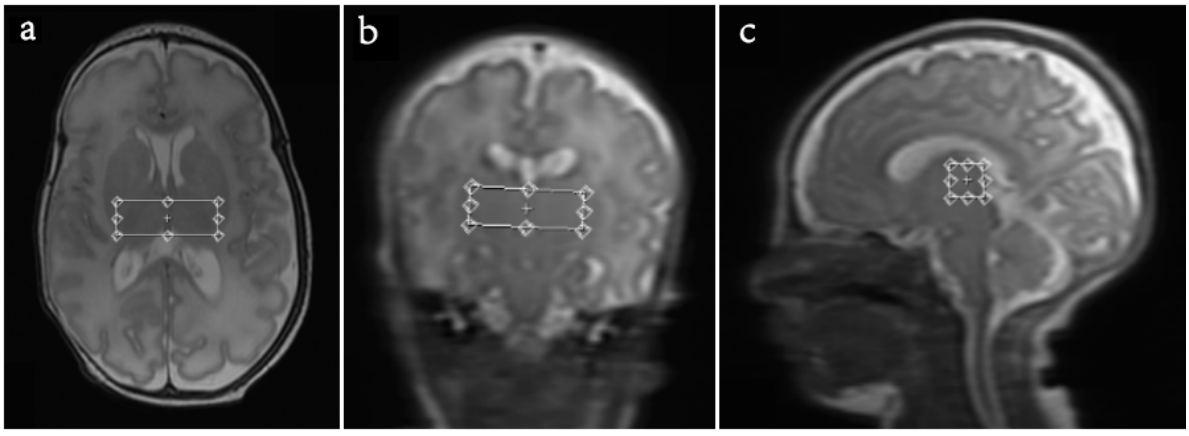

Figure 3: Placement of Voxel for SVS

3.3 LC Model

Quantification of brain metabolite concentrations was obtained through the use of the LCModel data analysis package (Stephen Provencher Inc., Oakville, Ontario, Canada, LCModel Version 6.3-0B). The LCModel method analyzes an *in vivo* spectrum as a **L**inear **C**ombination of model spectra of metabolite solutions *in vitro*. By using complete model spectra, rather than individual resonances, maximum information and uniqueness are incorporated into the analysis. A constrained regularization method accounts for differences in phase, baseline, and lineshapes between the *in vitro* and *in vivo* spectra, and estimates the metabolite concentrations and their uncertainties[21].

A major issue with the quantification of *in vivo* spectra has been parameterized models for peak distortion and for the baseline, which are too complicated to specify *a priori*. Empirical models with too few parameters have the potential to introduce bias, while too many parameters can produce artifacts and instabilities in the analysis. Both situations cause errors in the estimates. To avoid this, LCModel uses a nearly model-free constrained regularization method (developed by Steven Provencher in 1982), which attempts to choose the best compromise between these two situations by finding the smoothest lineshape and baseline that are consistent with the data[21].

One advantage of using LCModel is that because phasing, referencing, and quantification are done automatically, the results are user-independent, thus improving objectivity and thereby improving comparisons of different sets of results within and between laboratories. An example of the output from LCModel fitting is given in Figure 4 [21].

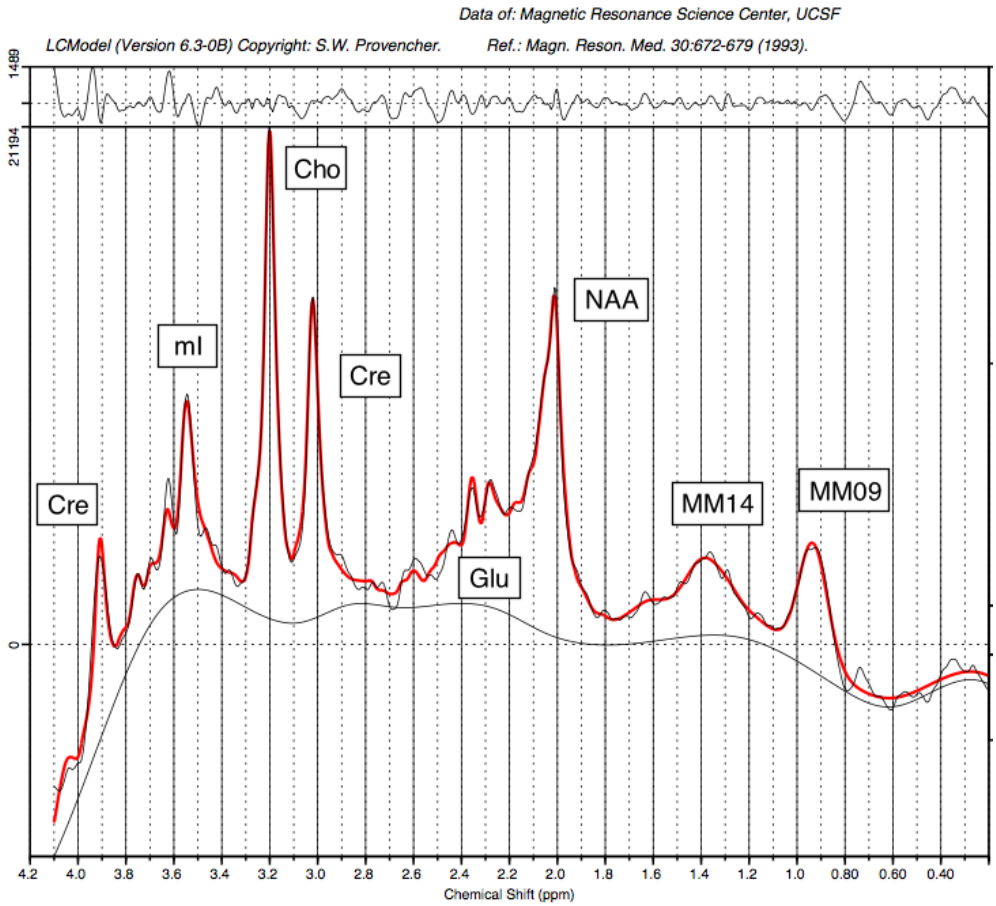

Figure 4: Example of LC Model Output

The black line is the frequency spectrum of the raw data, and the red line is the automated fit, processed from an appropriately defined "basis set" of simulated data. Labels for the peaks corresponding to the metabolites Creatine (Cre), the Glutamine+Glutamate complex (Glx), Myo-Inositol (mI), Choline, and N-Acetyl Aspartate (NAA) have been added for clarity. MM stands for macromolecules. MM09 represents signal from CH_3 groups on macromolecules with a chemical shift value of 0.9 ppm. Similarly, MM14 is the concentration of the CH_2 macromolecule peak near 1.4 ppm, which may also contain lipid contributions.

In order to add SVS data from 19 scans available for analysis that were acquired using a TE of 30ms, a new simulated expected spectrum ("basis set") was created to simulate peaks at TE=30ms. Because a TE-specific basis set was used, quantification of this spectroscopic data is thought to be comparable to the TE=35ms data.

3.4 Data Quality

The LC Model processing package contains a built-in data quality check. Cramér-Rao lower bounds, expressed as a percentage of the estimated concentrations, are provided as an estimate of the fitting error or statistical uncertainty. These are calculated using the residual error and the Fisher matrix of the partial derivatives of the concentrations[24]. As recommended in the LCModel Manual[25], only results with $\leq 15\%$ SD were included for statistical analysis. This eliminated 20 of 71 available scans from the data set. The signal-to-noise ratios (SNR) of the data included in analysis ranged from 11 to 66, and the mean SNR was 26.40 ± 9.22. Three data sets had a peak width measured at the full width half maximum (FWHM) greater than 0.1 ppm, and were therefore excluded from analysis. The resulting data set had an average peak width of 0.052 ± 0.016 ppm.

3.5 Statistical Analysis

For analysis, the ratio of mI to Cre was taken within each scan. This is because creatine concentration is reflective of metabolism, and has been demonstrated to be fairly constant[26]. Comparing the ratios, rather than the absolute concentrations, provides an internal normalization, which reduces intra-scan differences[27]. These concentration ratios were assessed in all patients (n=27) using mixed-effect linear models. Use of the mixed-effect model allowed us to address both inter-subject effects and intra-subject changes between serial MR examinations, by permitting multiple measurements per subject, thereby increasing statistical power.

4 Results

4.1 Changes with Age

NAA/Cho results for all cases without cerebellar hemorrhage (CbH) are shown in Figure 5. Using the calculated t-value of 3.9081 and 14 degrees of freedom, the two-tailed p-value is 0.0016, which is considered to be very statistically significant[28]. This is consistent with previously published data[29][13][30][18][8].

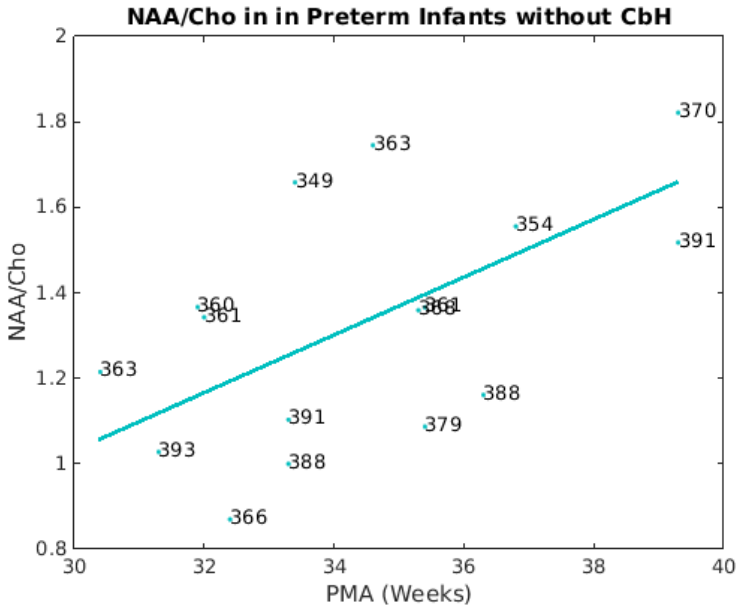

Figure 5: NAA/Cho Changes with Age in Premature Newborns without CbH

Cho/Cre results for all cases without CbH are shown in Figure 6. Using the calculated t-value of -2.2186 and 14 degrees of freedom, the two-tailed p-value is 0.0436, which is considered to be statistically significant[28]. This is consistent with previously published data[13][18][8].

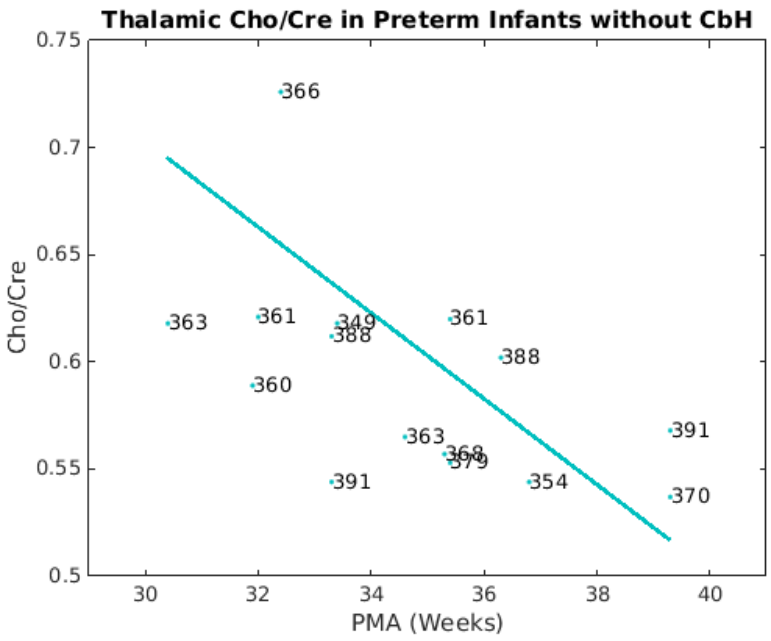

Figure 6: Cho/Cre Changes with Age in Premature Newborns without CbH

mI/Cre results for all cases without cerebellar hemorrhage (CbH) are shown in Figure 7. Using the calculated t-value of -2.4965 and 14 degrees of freedom, the two-tailed p-value is 0.0256, which is considered to be statistically significant. [28]

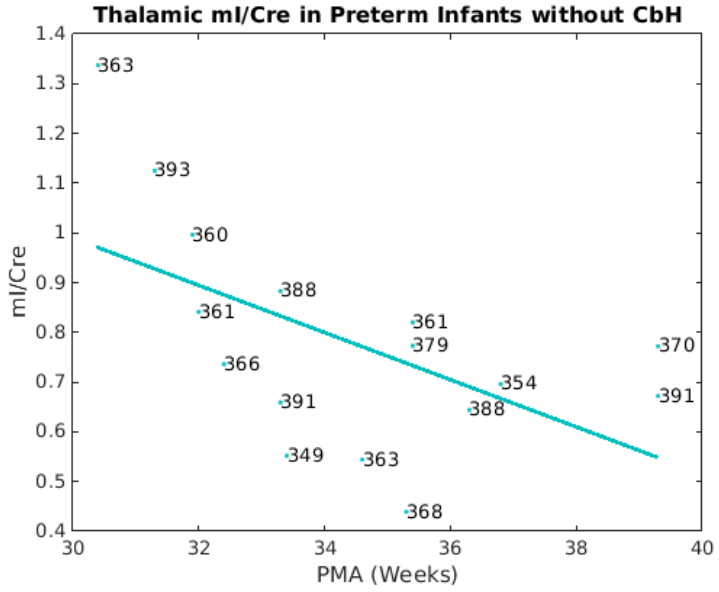

Figure 7: mI/Cre Changes with Age in Premature Newborns without CbH

5 Discussion

5.1 Implications

The changes in metabolism in the human brain during gestational age of 29-40 weeks reflect the fact that this is a critical period of rapid growth and development, when molecular and cellular processes are rapidly changing. These changes are a crucial aspect of developmental processes during early life, but they may also cause the perinatal brain to be more vulnerable to damage and the adverse symptoms of injury. The increase of NAA/Cre with age over the pre-term period is consistent with previously published data [18][30], and likely reflects increasing neuronal and axonal density and increasing neuronal activity[13][8]. This increase in density is likely indicative of the first stages of myelination and axonal elongation, which are key elements of early brain development. The decrease of Cho/Cre is also consistent with previously published findings [18], and may reflect a decrease in cell turnover. As Cho is abundant during cell membrane and de novo myelin synthesis[8], a decrease in total Cho concentration may signal the slowing of apoptosis and cell turnover, as developing oligodendrocytes and Schwann cells begin to stabilize.

In this study, a baseline pattern of mI concentration changes over the course of normal preterm development has been established. The decrease in mI is consistent with previous findings of a decrease in mI concentration from birth to 3 months of age [18]. This decrease may be due to a reduction in cell turnover, as a reduction in apoptosis associated with cell turnover would reduce the overall concentration of mI due to a decrease in mI concentration in the extracellular compartment. Additionally, this decrease could be interpreted as a signal of early myelin maturation, as mI is thought to be a marker of immature myelination[8]. Further investigation both *in vivo* and *in vitro* could help confirm or refute these explanations.

5.2 Limitations

There are several challenges in acquisition of MRI data in such small patients. First, even under sedation, infants tend to move over the duration of their MR exams. This can cause visually apparent motion artifacts in anatomical imaging, but more subtle artifacts can also occur in spectroscopy. The data-quality thresholding used in this study is an effort to reduce the effect of such artifacts, but there may be residual errors in the included data, such as slightly increased linewidths, overall frequency shifts, and possibly reduced peak areas due to phase cancellation[31]. Second, the size of the region of interest (ROI) is pre-determined, in order to give consistent SNR and to allow for direct comparison of results. However, some of the youngest patients enrolled in this study had such small thalami when they were scanned that there could have been appreciable partial volume effects, wherein some signal from the surrounding structures, such as the basal ganglia or the ventricles, was included in the spectrum. If a partial volume of CSF was included, for example, a peak at 1.3 ppm corresponding to lactate appeared in the spectrum, which would not be expected in normal thalamic tissue[15][32]. This occurred in many of the scans included for analysis, but it was accounted for in processing, and had no effect on the other metabolites measured.

Of the 22 subjects who have reached a corrected gestational age of 1 year, cognitive, language and motor scoring has been obtained for 12 of them. Of these, only 6 of their short-TE spectroscopic data was of sufficient quality to be included in analysis, and so this sample size is too small to perform a meaningful group analysis. However, we expect to eliminate this statistical limitation with time, as data collection is ongoing.

6 Future Work

In order to gain a more detailed understanding of metabolic changes across development, three-dimensional Magnetic Resonance Spectroscopic Imaging (MRSI) will be needed, so that metabolite concentrations can be more accurately localized to various brain regions and

tissue types. As the study progresses, additional participants will be enrolled and tested, increasing the availability of neurological follow-up information. Therefore, we expect an in-depth analysis of metabolic changes with regard to cognitive, language, and motor scores to become possible in the future.

References

[1] Eunice Kennedy Shriver National Institute of Child Health and Human Development. *Preterm Labor and Birth: Overview*. 2014. URL: http://www.nichd.nih.gov/health/topics/preterm/Pages/default.aspx (visited on 02/05/2015).

[2] Centers for Disease Control and Prevention. *Preterm Birth*. 2014. URL: http://www.cdc.gov/reproductivehealth/maternalinfanthealth/PretermBirth.htm (visited on 02/15/2015).

[3] World Health Organization. *Fact Sheet No 363*. 2014. URL: http://www.who.int/mediacentre/factsheets/fs363/en/ (visited on 04/16/2015).

[4] Imad T. Jarjour. "Neurodevelopmental Outcome After Extreme Prematurity: AReview of the Literature". In: *Pediatric Neurology* 52.2 (2015), pp. 143 –152. ISSN: 0887-8994. DOI: http://dx.doi.org/10.1016/j.pediatrneurol.2014.10.027. URL: http://www.sciencedirect.com/science/article/pii/S0887899414006584.

[5] Joann S. Poh et al. "Developmental synchrony of thalamocortical circuits in the neonatal brain". In: *NeuroImage* (2015). ISSN: 1053-8119. DOI: http://dx.doi.org/10.1016/j.neuroimage.2015.03.039. URL: http://www.sciencedirect.com/science/article/pii/S1053811915002219.

[6] Andrea S Kierans et al. "Myoinositol and glutamate complex neurometabolite abnormality after mild traumatic brain injury". In: *Neurology* 82.6 (2014), pp. 521–528.

[7] Maria Erecinska, Shobha Cherian, and Ian A Silver. "Energy metabolism in mammalian brain during development". In: *Progress in neurobiology* 73.6 (2004), pp. 397–445.

[8] Andrew J Degnan et al. "Early metabolic development of posteromedial cortex and thalamus in humans analyzed via in vivo quantitative magnetic resonance spectroscopy". In: *Journal of Comparative Neurology* 522.16 (2014), pp. 3717–3732.

[9] Steven P. Miller et al. "Patterns of brain injury in term neonatal encephalopathy". In: *The Journal of Pediatrics* 146.4 (2005), pp. 453 –460. ISSN: 0022-3476. DOI: http://dx.doi.org/10.1016/j.jpeds.2004.12.026. URL: http://www.sciencedirect.com/science/article/pii/S0022347604011783.

[10] Hirohiko Kimura et al. "Metabolic Alterations in the Neonate and Infant Brain during Development: Evaluation with Proton MR Spectroscopy". In: *Radiology* 194 (1995), pp. 483–489.

[11] Jun-ichi Takanashi et al. "Metabolic Changes in Early Childhood Using LCModel With Corrected Water Scaling Method". In: *Journal of Magnetic Resonance Imaging* 35 (2012), pp. 174–180.

[12] José M Pascual et al. "Time course of early metabolic changes following diffuse traumatic brain injury in rats as detected by 1H NMR spectroscopy". In: *Journal of neurotrauma* 24.6 (2007), pp. 944–959.

[13] Ashok Panigrahy, Marvin D Nelson Jr, and Stefan Blüml. "Magnetic resonance spectroscopy in pediatric neuroradiology: clinical and research applications". In: *Pediatric radiology* 40.1 (2010), pp. 3–30.

[14] Stephen K Fisher, James E Novak, and Bernard W Agranoff. "Inositol and higher inositol phosphates in neural tissues: homeostasis, metabolism and functional significance". In: *Journal of Neurochemistry* 82.4 (2002), pp. 736–754.

[15] Stephen Ashwal et al. "Proton Spectroscopy Detected Myoinositol in Children with Traumatic Brain Injury". In: *Pediatric Research* 56.4 (Oct. 2004), pp. 630–638. URL: http://dx.doi.org/10.1203/01.PDR.0000139928.60530.7D.

[16] Mohammad Haris et al. "In vivo Mapping of Brain Myo-Inositol". In: *Neuroimage* 54.3 (2011), pp. 2079–2085.

[17] Rui V Simões et al. "Brain metabolite differences in one-year-old infants born small at term and association with neurodevelopmental outcome". In: *American journal of obstetrics and gynecology* (2015).

[18] Stefan Blüml et al. "Metabolic maturation of the human brain from birth through adolescence: insights from in vivo magnetic resonance spectroscopy". In: *Cerebral Cortex* 23.12 (2013), pp. 2944–2955.

[19] Morris H Baslow. "Functions of N-Acetyl-l-Aspartate and N-Acetyl-l-Aspartylglutamate in the Vertebrate Brain". In: *Journal of neurochemistry* 75.2 (2000), pp. 453–459.

[20] *Prematurely born neonate MRI (PreMRI)*. URL: http://www.radiology.ucsf.edu/research/labs/baby-brain/premri.

[21] Stephen W. Provencher. "Estimation of metabolite concentrations from localized in vivo proton NMR spectra". In: *Magnetic Resonance in Medicine* 30.6 (1993), pp. 672–679. ISSN: 1522-2594. DOI: 10.1002/mrm.1910300604. URL: http://dx.doi.org/10.1002/mrm.1910300604.

[22] Jason C. Crane, Marram P. Olsons, and Sarah J. Nelson. "SIVIC: Open-Source, Standards-Based Software for DICOM MR Spectroscopy Workflows". In: *International Journal of Biomedical Imaging* 2013 (2013), p. 12. DOI: http://dx.doi.org/10.1155/2013/169526. URL: sivic.sourceforge.net.

[23] Sandeep K. Ganji et al. "T2 measurement of J-coupled metabolites in the human brain at 3T". In: *NMR in Biomedicine* 25.4 (2012), pp. 523–529. ISSN: 1099-1492. DOI: 10.1002/nbm.1767. URL: http://dx.doi.org/10.1002/nbm.1767.

[24] Gunther Helms. "The principles of quantification applied to in vivo proton {MR} spectroscopy". In: *European Journal of Radiology* 67.2 (2008). Clinical 1H {MR} Spectroscopy, pp. 218 –229. ISSN: 0720-048X. DOI: http://dx.doi.org/10.1016/j.ejrad.2008.02.034. URL: http://www.sciencedirect.com/science/article/pii/S0720048X08001411.

[25] Stephen Provencher. *LCModel & LCMgui Users Manual*. 2014.

[26] Carolyn E. Mountford et al. "Neurospectroscopy: The Past, Present and Future". In: *Chemical Reviews* 110.5 (2010), pp. 3060–3086. DOI: 10.1021/cr900250y. URL: http://dx.doi.org/10.1021/cr900250y.

[27] Antonin Skoch, Filip Jiru, and Jürgen Bunke. "Spectroscopic imaging: Basic principles". In: *European Journal of Radiology* 67.2 (2008), pp. 230–239.

[28] John C. Pezullo. *GraphPad P Value Calculator*. 2015. URL: `http://graphpad.com/quickcalcs/pValue2/` (visited on 05/28/2015).

[29] Daniel B Vigneron. "Magnetic resonance spectroscopic imaging of human brain development". In: *Neuroimaging Clinics of North America* 16.1 (2006), pp. 75–85.

[30] Duan Xu et al. "MR spectroscopy of normative premature newborns". In: *Journal of Magnetic Resonance Imaging* 33.2 (2011), pp. 306–311.

[31] Roland Kreis. "Issues of spectral quality in clinical ^{1}H-magnetic resonance spectroscopy and a gallery of artifacts". In: *NMR in Biomedicine* 17.6 (2004), pp. 361–381.

[32] Caroline D Rae. "A guide to the metabolic pathways and function of metabolites observed in human brain 1H magnetic resonance spectra". In: *Neurochemical research* 39.1 (2014), pp. 1–36.

A Appendix A: Extra Figures

NAA/Cho results for all cases (with and without CbH) are shown in Figure 8. Using the calculated t-value of 4.8838 and 31 degrees of freedom, the two-tailed p-value is less than 0.0001, which is considered to be extremely statistically significant[28]. This is consistent with previously published data[30][18][8] [13].

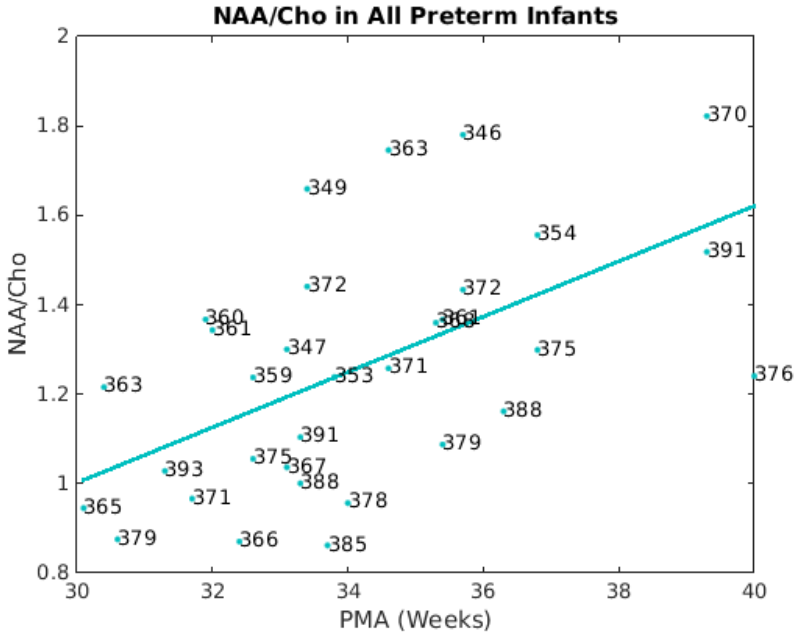

Figure 8: NAA/Cho Changes with Age in All Premature Newborns

Cho/Cr results for all cases (with and without CbH) are shown in Figure 9. Using the calculated t-value of -1.5927 and 31 degrees of freedom, the two-tailed p-value is 0.1214, which is considered to be not statistically significant. [28] However, the general trend of decreasing Cho/Cre is consistent with previously published data[13].

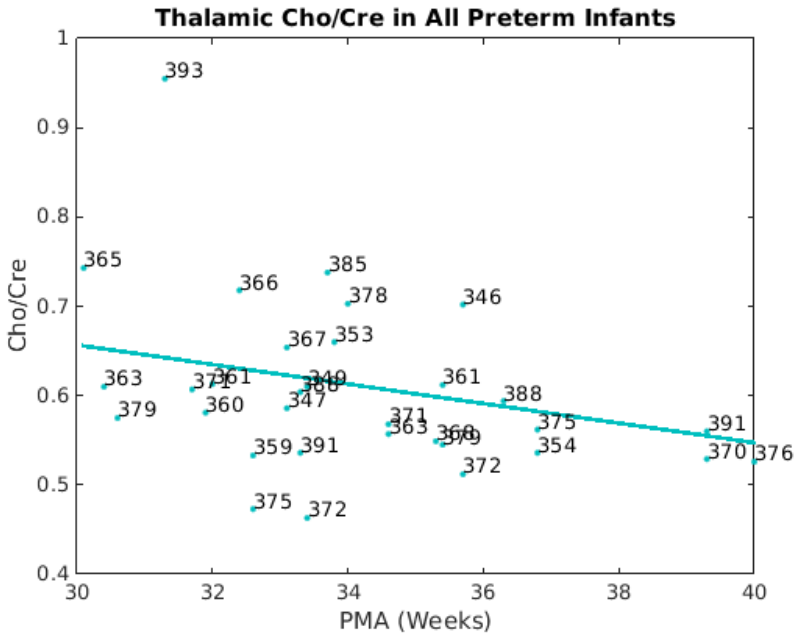

Figure 9: Cho/Cre Changes with Age in All Premature Newborns

mI/Cre results for all cases (with and without CbH) are shown in Figure 10. Using the calculated t-value of -2.0618 and 31 degrees of freedom, the two-tailed p-value is 0.0477, which is considered to be statistically significant. [28]

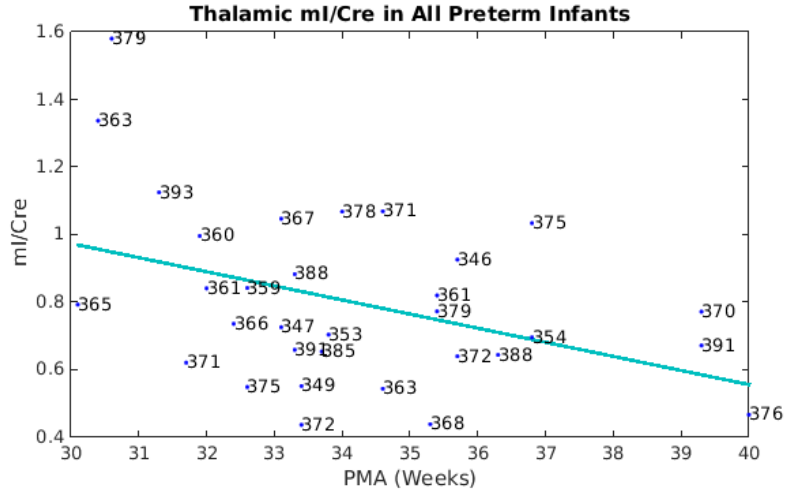

Figure 10: mI/Cre Changes with Age in All Premature Newborns

Publishing Agreement

It is the policy of the University to encourage the distribution of all theses, dissertations, and manuscripts. Copies of all UCSF theses, dissertations, and manuscripts will be routed to the library via the Graduate Division. The library will make all theses, dissertations, and manuscripts accessible to the public and will preserve these to the best of their abilities, in perpetuity.

Please sign the following statement:

I hereby grant permission to the Graduate Division of the University of California, San Francisco to release copies of my thesis, dissertation, or manuscript to the Campus Library to provide access and preservation, in whole or in part, in perpetuity.

Author Signature

Sept 2, 2015

Date